

# Type I Membranes, Phase Resetting Curves, and Synchrony

Bard Ermentrout \*  
Department of Mathematics  
University of Pittsburgh  
Pittsburgh, PA 15260

November 30, 1995

## Abstract

Type I membrane oscillators such as the Connor model (Connor, Walter, and McKown, 1977) and the Morris-Lecar model (Morris and Lecar, 1981) admit very low frequency oscillations near the critical applied current. Hansel et.al., (1995) have numerically shown that synchrony is difficult to achieve with these models and that the phase resetting curve is strictly positive. We use singular perturbation methods and averaging to show that this is a general property of Type I membrane models. We show in a limited sense that so called type 2 resetting occurs with models that obtain rhythmicity via a Hopf bifurcation. We also show the differences between synapses that act rapidly and those that act slowly and derive a canonical form for the phase interactions.

## 1 Introduction

The behavior of coupled neural oscillators has been the subject of a great deal of recent interest. In general, this behavior is quite difficult to analyze. Most of the results to date are primarily based on simulations of specific models. One of the main questions that is asked is whether two identical oscillators will synchronize if they are coupled or whether they will undergo other types of behavior. In a recent paper, van Vreeswijk, et al (1995) show

---

\*Supported in part by NSF DMS-93-03706 and by NIMH-47150

that the timing of synapses is very important in determining whether, say, excitatory synaptic interactions will lead to synchronous behavior. Hansel *et.al.* (1995) contrast the behavior of weakly coupled neural oscillators for different membrane models. They find substantial differences between standard Hodgkin-Huxley models and Connor models (Connor, *et al* 1977) which have the additional A current.

One easily measurable property of a neural oscillator (either an experimental system or a simulated one) is its phase resetting curve. The phase resetting curve or PRC is found by perturbing the oscillation with a brief depolarizing stimulus at different times in its cycle and measuring the resulting phase-shift from the unperturbed system. By making the perturbation infinitesimally small (in duration and amplitude), it is possible (at least for the simulated system) to derive what is called in Kuramoto (1981) and Hansel, *et.al.* (1993,1995) the *response function* of the neural oscillator. Thus, Hansel and collaborators show that the response function or infinitesimal PRC for the Connor model is very different from that of the Hodgkin-Huxley model. In particular, they show that perturbations of the Connor model can *never* delay the onset of a spike; only advance it. That is, the phase resetting curve for the Connor model is non-negative. In contrast, the PRC of the Hodgkin-Huxley model has both negative and positive regions. They refer to models with strictly positive phase resetting curves as “Type I” and those for which the phase resetting curve has a negative regime as “Type II.”

The differences in the response of the oscillators to brief stimuli have profound consequences for coupled cells. In particular, Hansel *et al* (1995) show that excitatory synapses cannot lead to synchronization for the Connor model. Their result is quite general, in that they explore the consequences of type I phase resetting on coupling without reference to a particular model. In particular, they show that unless the synapses are very fast, synchrony for excitatory coupling is not possible. Their results are similar to those obtained by van Vreeswijk, *et. al.* for integrate and fire cells and the Hodgkin-Huxley model.

The goal of this paper is to demonstrate that the differences between Hodgkin-Huxley type oscillators and the Connor model can be accounted for by looking at the mechanism by which the membranes go from resting to repetitive firing as current is injected. We use a singular perturbation method to derive the response of the membrane to weak inputs such as brief pulses of current and synaptic drive. From these calculations, we derive a “canonical” form for both the phase resetting curve and the phase interaction function for coupled membrane oscillators that are similar to the Connor

model. We use this to compute the stability of synchrony and anti-phase activity as a function of the temporal properties of the synapses.

In Rinzel and Ermentrout (1989) we review the classification of excitable membranes by Hodgkin (1948) in terms of their dynamics as a current is injected. There are two main types of excitable axons: Type I and Type II. (Henceforth, in order to avoid confusion between the classification of membrane excitability and phase resetting curves, we will always say “Type I PRC” when referring to phase resetting curves and “Type I membrane” or “Type I excitability” when referring to dynamics of the membrane.) Type I membranes are characterized mainly by the appearance of oscillations with arbitrarily low frequency as current is injected whereas for Type II membranes, the onset of repetitive firing is at a nonzero frequency. The Connor model is an example of Type I excitability. In Figure 1a, we show the frequency as a function of injected current for the Connor model and for contrast, the current-frequency response for the Hodgkin-Huxley model (a Type II membrane) is shown in Figure 1b. The repetitive activity first occurs at a nonzero frequency for the Hodgkin-Huxley model (that is the minimum firing rate is greater than zero.) The minimal firing rate of the Connor model is zero.

The difference between these two models arises in the mechanism by which repetitive firing ensues. In “Type II” membranes, like the Hodgkin-Huxley, the following occurs: For low currents, there is a single equilibrium state and it is asymptotically stable. As the current increases, this state loses stability via a (subcritical) Hopf bifurcation and repetitive firing ensues. By contrast in “Type I” membranes such as the Connor model, there are three equilibria for currents below the critical current: a low voltage one that is stable (E), a high voltage one which is unstable and an intermediate voltage equilibrium which is an unstable saddle point (S). The saddle point plays a pivotal role in the onset of repetitive firing. It has one positive eigenvalue and the remaining eigenvalues have negative real parts. There is a pair of trajectories that leave the saddle point (the “unstable manifold”) and enter the stable fixed point. Together these two trajectories form a loop in the phase-space. This is illustrated schematically in Figure 2. In the phase-space for the equations (six dimensional for the Connor model) there is a closed loop which contains two fixed points: the stable rest point and the unstable saddle-point. As the current increases, these two fixed points merge and disappear leaving a stable periodic solution – the repetitive firing. In order to shed light on the phase resetting function and the behavior of coupled neurons, we will concentrate on parameter values near the critical current

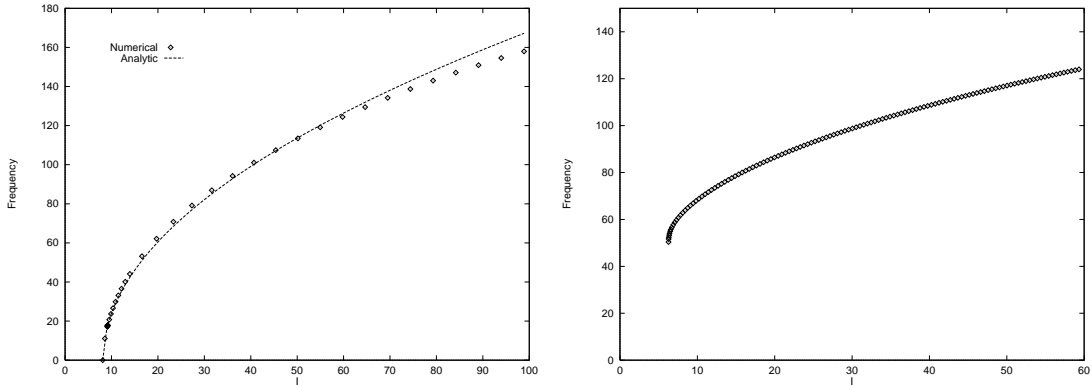


**Figure 1:** Frequency as a function of injected current for two different membrane models (a) Connor ; (b) Hodgkin-Huxley. (Note that a formula for the frequency as derived from asymptotics in section 2 is also shown for the Connor model.)

for which the two rest states coalesce. The reason for this restriction is that we can explicitly work out the complete nonlinear behavior near criticality.

Numerical calculations near criticality are quite difficult for the Connor model due to its high dimension. Furthermore, near the critical current, the Connor model has 5 rather than 3 fixed points (only one of which is stable) and this appears to complicate the application of the present analysis to that model. A simpler model that behaves in much the same way as either the Hodgkin-Huxley equations or the Connor model (depending on the chosen parameters) is the Morris-Lecar model (Morris and Lecar, 1981, Rinzel and Ermentrout, 1989). The dimensionless equations are

$$\begin{aligned} \frac{dV}{dt} &= I - g_l(V - V_L) - g_K w(V - V_k) - g_{Ca} m_\infty(V)(V_{Ca} - V) \\ \frac{dw}{dt} &= \lambda(V)(w_\infty(V) - w) \end{aligned}$$

where

$$\begin{aligned} m_\infty(V) &= .5(1 + \tanh((V - V_1)/V_2)) \\ w_\infty(V) &= .5(1 + \tanh((V - V_3)/V_4)) \\ \lambda(V) &= \frac{1}{3} \cosh((V - V_3)/(2V_4)). \end{aligned}$$

(The values of the parameters are found in the Appendix.) We will use this simpler model to illustrate the asymptotics. In the “Type I” excitabil-

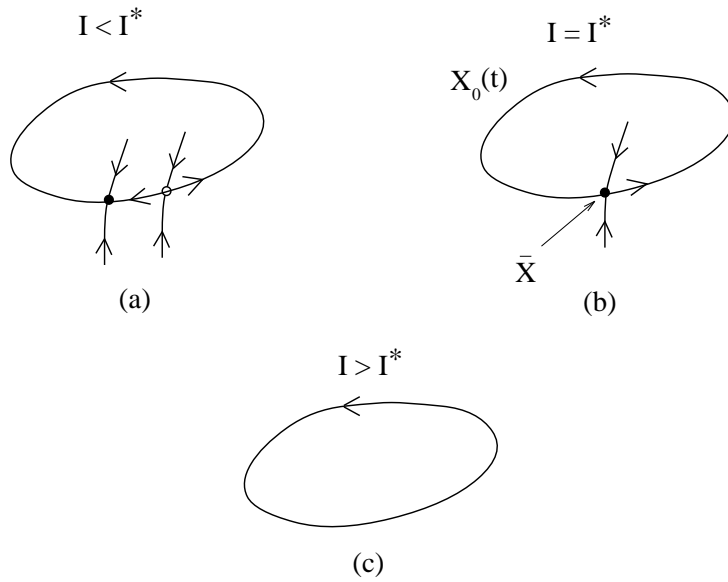


**Figure 2:** Saddle-node bifurcation on an invariant circle as the applied current,  $I$  varies. (a) For  $I < I^*$  there is a unique asymptotically stable fixed point and a saddle-point with a 1-dimensional unstable manifold whose branches form a closed loop. (b) At criticality,  $I = I^*$  the node and the saddle coalesce at the point  $\bar{X}$  forming a simple loop,  $X_0(t)$ . (Here,  $X$  is the vector of coordinates for the single membrane oscillator.) (c) For  $I > I^*$  all that remains is a stable limit cycle.

ity regime as  $I$  varies from a low to a high value, there is a saddle-node bifurcation on the circle leading to sustained slow oscillations.

As we mentioned at the outset of this paper, one of our goals is to characterize the response of neural oscillators to stimuli. In particular, like Hansel, et al (1995), we will examine the phase resetting curve for different types of membrane oscillators. In figure 3a,b, we show the infinitesimal PRC or response function for the Connor model and for the Hodgkin-Huxley model. As noted by Hansel et. al. (1995), they are quite different. The Connor model is strictly positive and as a consequence brief stimuli can only advance the oscillator. There is a large negative region for the Hodgkin-Huxley model which implies that it is possible to delay the firing of an action potential by an appropriately timed stimulus. Figure 3c shows the same functions for the Morris-Lecar equations in the “type I” and “type II” excitability regimes. This suggests that the differences lie not in time constants of various currents, but rather in the mechanisms leading to repetitive firing.

The PRC of Type I membranes and their behavior with weak coupling is in a sense universal. That is, near the critical current all of these models have a similar nature if the coupling is small. Ultimately, we have the rather pleasant result that “Type I membranes have Type I phase resetting curves.” Thus, the remainder of this paper is devoted to showing why this is true and what the consequences are for synaptic coupling of such oscillators.

## 2 The solution and response function near the bifurcation.

The membrane potential for a typical synaptically coupled membrane model satisfies:

$$C \frac{dV}{dt} = -I_{ionic} + I + \hat{g}_{syn} s(t) (V_{syn} - V) \quad (2.1)$$

where  $I_{ionic}$  are the ionic conductances,  $I$  is the applied current, and  $\hat{g}_{syn}$  is the maximal synaptic conductance. The function  $s(t)$  is the fraction of open channels due to the firing of a presynaptic neuron. There are numerous ways to model the synaptic conductance. It can satisfy a system of differential equations based on the presynaptic potential (as in Destexhe, *et al*, 1994) or more simply be an “alpha function,”  $s(t) = \alpha^2 t e^{-\alpha t}$ . In the former case, if  $V_{pre}(t)$  is the potential of the presynaptic cell, then  $s(t)$  satisfies:

$$\frac{ds}{dt} = \alpha k (V_{pre}) (1 - s) - \beta s \quad (2.2)$$

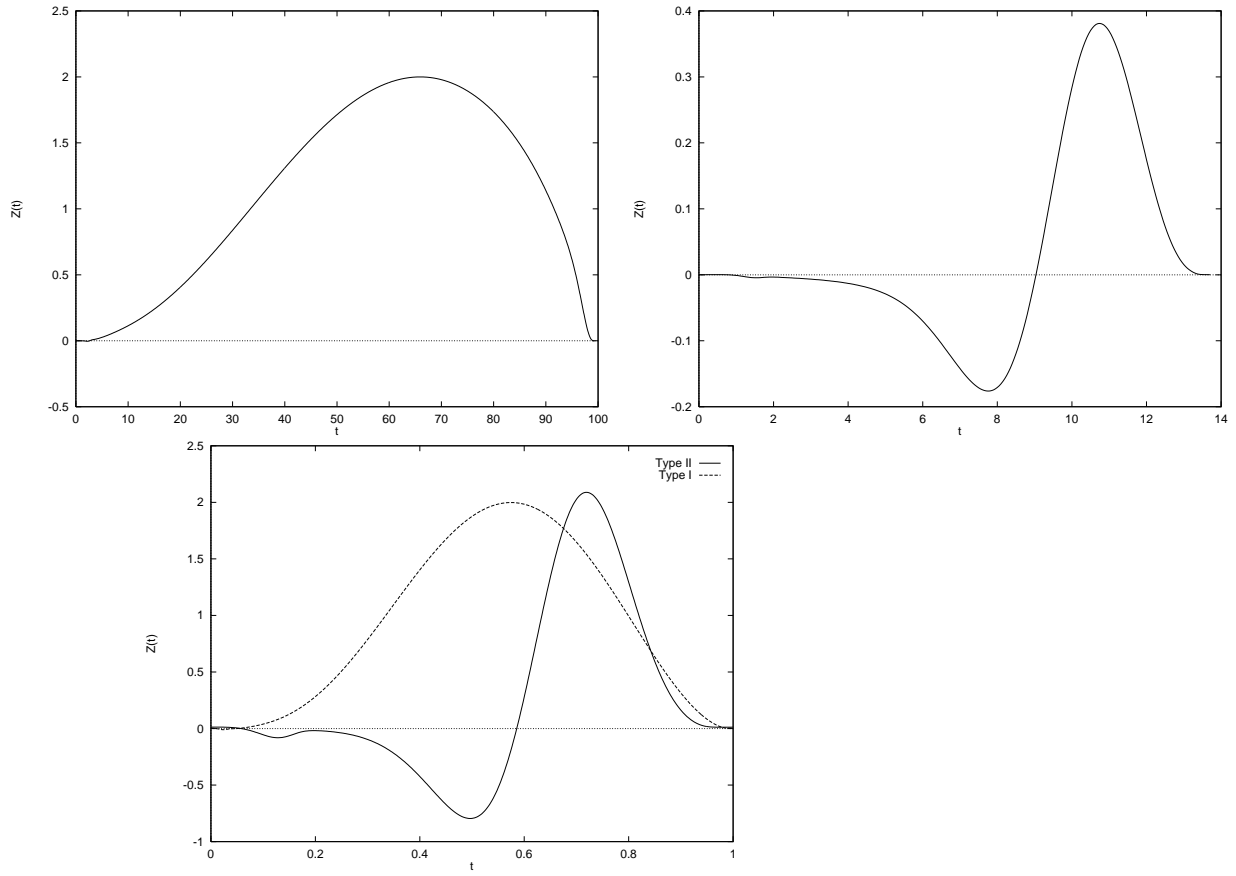


**Figure 3:** Response functions for membrane oscillators: (a) Connor model. (b) Hodgkin-Huxley model. (c) Morris-Lecar model in two different regimes. (Note: In (c)  $Z(t)$  and  $t$  have been scaled to the same ranges.)

where  $\alpha, \beta$  are constants and  $k$  is a saturating threshold function, such as  $k(v) = 1/(1 + \exp(-(v - v_{thr})/v_s))$ . For  $v_s$  small, this is like a Heaviside step-function.

Recall that for Type I excitable membranes, the onset of repetitive firing occurs when a saddle point and a stable node coalesce (*cf* Figure 2.) At this critical current, there is a trajectory leaving the saddle-node point from one side and entering it from the other. Let  $X \equiv (V, m, h, \dots)$  denote the vector of variables for the single membrane oscillator. Let  $I^*$  be the critical value for the current. Let  $\bar{X}$  be the saddle-node point and let  $X_0(t)$  denote the closed “infinite period” trajectory containing  $\bar{X}$ . That is

$$\lim_{t \rightarrow \pm\infty} X_0(t) = \bar{X}.$$

## 2.1 The periodic solution

Before we add synaptic currents, it is easier to first examine a constant current scaled by a small positive parameter,  $\epsilon^2$ . The equations for the voltage are:

$$C \frac{dV}{dt} = -I_{ionic} + I^* + \epsilon^2 i.$$

If  $i > 0$  then the phase space will be as in Figure 2c (since  $I = I^* + \epsilon^2 i$ .) If  $i < 0$  then there will be a saddle-node pair as in Figure 2a.

More generally, consider the equations:

$$\frac{dX}{dt} = F_0(X) + \epsilon^2 N(X). \quad (2.3)$$

We assume that when  $\epsilon = 0$  there is a saddle-node bifurcation at the point  $X = \bar{X}$ . We write the Taylor expansion for  $F_0(X)$  around this point:

$$F_0(X) = A(X - \bar{X}) + Q(X - \bar{X}, X - \bar{X}) + \dots \quad (2.4)$$

where  $A$  is the Jacobian matrix of  $F_0$  evaluated at  $\bar{X}$  and  $Q$  is the quadratic term of the Taylor series. By assumption ( $X = \bar{X}$  is a saddle-node point)  $A$  is a singular matrix. That is, it has a zero eigenvalue. We will assume (generically) that this zero is simple. Let  $\vec{e}$  be the unit eigenvector of  $A$  having zero eigenvalue and let  $\vec{f}$  be the eigenvector of  $A^T$  satisfying  $\vec{f} \cdot \vec{e} = 1$ . Let  $X(t) = \bar{X} + \epsilon z \vec{e} + \dots$  where  $z$  is a scalar quantity that depends on time. In Ermentrout and Kopell (1986) we show that the dynamics of (2.3) are governed by those of  $z$  which are:

$$\frac{dz}{dt} = \epsilon(\eta + qz^2) + \dots \quad (2.5)$$



where

$$\eta = \vec{f} \cdot N(\bar{X})$$

and

$$q = \vec{f} \cdot Q(\vec{e}, \vec{e}).$$

Both of these quantities are easily computed for membrane models. In particular,  $\eta$  is directly proportional to  $i$  while  $q$  depends on the details of the membrane model used. If  $\eta$  and  $q$  have opposite signs then (2.5) has a pair of fixed points, one stable and one unstable corresponding to fixed points of (2.3) or (2.1). On the other hand, if  $\eta$  and  $q$  have the same sign, say, positive, then the lowest order solution to (2.5) is

$$z(t) = \sqrt{\frac{\eta}{q}} \tan(\epsilon \sqrt{\eta q} (t - c))$$

where  $c$  is an arbitrary constant. Notice that  $z$  is “periodic” but that it “blows up” since the tangent function has singularities at odd multiples of  $\pi/2$ . In Ermentrout and Kopell (1986), we show that “blowing up” of this reduced system corresponds to producing a spike for the full system, (2.3). Thus, the period of the full equations is:

$$T = \frac{\pi}{\epsilon \sqrt{\eta q}}.$$

For the membrane model, since,  $I = I^* + \epsilon^2 i$ , the period of the membrane oscillator is:

$$T_{mem} = C \frac{1}{\sqrt{I - I^*}}$$

where  $C$  is a constant that depends on the details of the model. This short calculation shows a general property of Type I membranes. The frequency is proportional to the square root of the difference between the applied current and the critical current. (*Note.* In the paper by Connor, et.al. (1977), the authors attempt to fit the frequency with a straight line. It is much better fitted with a square-root function, e.g.  $17.553\sqrt{I - 8.114}$ . See Figure 1a.)

The “blow-up” of a solution is an indication that equation (2.3) is *singularly* perturbed as  $\epsilon$  tends to zero. Thus, in general, one attempts to “match” the solution of (2.3) to (2.5) when  $\epsilon \rightarrow 0$ . This matching is fairly straightforward so we do not perform the details here. For later use, the solution in terms of normal time is:

$$X(t) = X_0(t) + \epsilon \left( z(t) - \frac{1}{\frac{\pi}{2} - \sqrt{\eta q} \epsilon t} - \frac{1}{-\frac{\pi}{2} - \sqrt{\eta q} \epsilon t} \right) \vec{e}. \quad (2.6)$$

For the membrane model,  $\eta = ci$  where  $c$  is a model-dependent constant. Note that as  $\sqrt{\eta q} \epsilon t \rightarrow \pm\pi/2$  the solution, (2.6) is well defined as we have subtracted the singularity of the tangent function away. (Recall from calculus that

$$\lim_{x \rightarrow \pi/2^-} \tan(x) - 1/(\pi/2 - x) = 0$$

so  $X(t)$  is defined and periodic for  $\sqrt{\eta q} \epsilon t \in [-\pi/2, \pi/2]$ .)

## 2.2 A convenient change of variables and the response function

The formula (2.6) gives the full behavior of a single membrane oscillator when perturbed into the regime of repetitive firing. Similarly, the “firing time” of the membrane oscillator is found from the solution to (2.5). In order to study the effects of coupling and the phase resetting curve for the system, it is convenient to change to a phase equation. In the same manner as Ermentrout and Kopell (1986) we rescale time as  $\tau = \epsilon t$  and let

$$z = \tan(\theta/2).$$

Then (2.5) becomes

$$\frac{d\theta}{d\tau} = q(1 - \cos \theta) + (1 + \cos \theta)\eta. \quad (2.7)$$

This is a form of “phase equation” which describes the single oscillator in terms of an angle variable that lies between  $-\pi$  and  $\pi$ . Each time  $\theta = \pi$  the full model fires a spike. The constant  $\eta$  is proportional to the *applied current* as well as any *synaptic current*. In particular, suppose a constant positive current is applied,

$$\eta = ci$$

where  $c, q$  are both positive. (These constants depend on the details of the model.) Then (2.7) is easy to solve by quadrature:

$$\theta(t) = 2 \tan^{-1} \left( \sqrt{\frac{ci}{q}} \tan(\sqrt{icq} \tau + \xi) \right)$$

where  $\xi$  is an arbitrary phase shift. The phase monotonically increases and covers one period in  $\pi/\sqrt{icq}$  *slow* time units. (Recall, the slow time  $\tau = \epsilon t$ .) To compute the phase resetting curve, one just briefly increments the bias

current, *i*. Hansel, *et al* (1995) compute the *infinitesimal* phase resetting curve which arises when the amplitude of the perturbation tends to zero. For the present model, since it is a scalar differential equation, it is easy to compute the infinitesimal PRC (see Appendix B for the calculation):

$$\Delta(\theta) = K(1 + \cos \theta) \tag{2.8}$$

where  $K$  is a constant related to the amplitude of the stimulus. The actual PRC is any phase-shift of (2.8); here we have shifted it so that the spike occurs at  $\theta = \pi$ . Summarizing, we have shown that *Every type I membrane oscillator near the critical current has a nonnegative PRC that is close to (2.8) in shape. In particular, the infinitesimal phase resetting curve is non-negative.*

In Figures 4a and 4b we depict the infinitesimal PRC for the Morris-Lecar model in the “Type I” excitability regime near criticality as well as that for the Connor model. Plotted along with these two curves is the formula (2.8) with the appropriate choice of  $K$  and the appropriate phase-shift. The PRC computed from (2.8) is nearly indistinguishable from that of the Morris-Lecar model. The Connor model is qualitatively similar but not as close as the Morris-Lecar model. Similar calculations with other models such as a variant of Hodgkin-Huxley described by Wang (X.J. Wang, personal communication) show a very close fit near criticality. We suspect that the reason that the asymptotics do not agree as well with the Connor model as they do with the Morris-Lecar lies in the numerical difficulties of computing the response function near criticality. One can decrement the time step for integration of the equations and in some cases that decreases the error in the numerical computation but in others increases it. Finally it is probable that the higher order corrections for the expansion of the response function for the Connor model are much larger than those of the Morris-Lecar.

The point of this calculation is that we now have a precise expression for the response function  $Z(t)$  for any membrane model near the saddle-node bifurcation, namely, (2.8). We also have an expression for the membrane potential. We now proceed to the behavior of these oscillators when they are synaptically coupled.

### 3 Coupled Type I Membranes.

The main purpose for computing the response function for an oscillator is so that we can study the behavior of such models when they are coupled

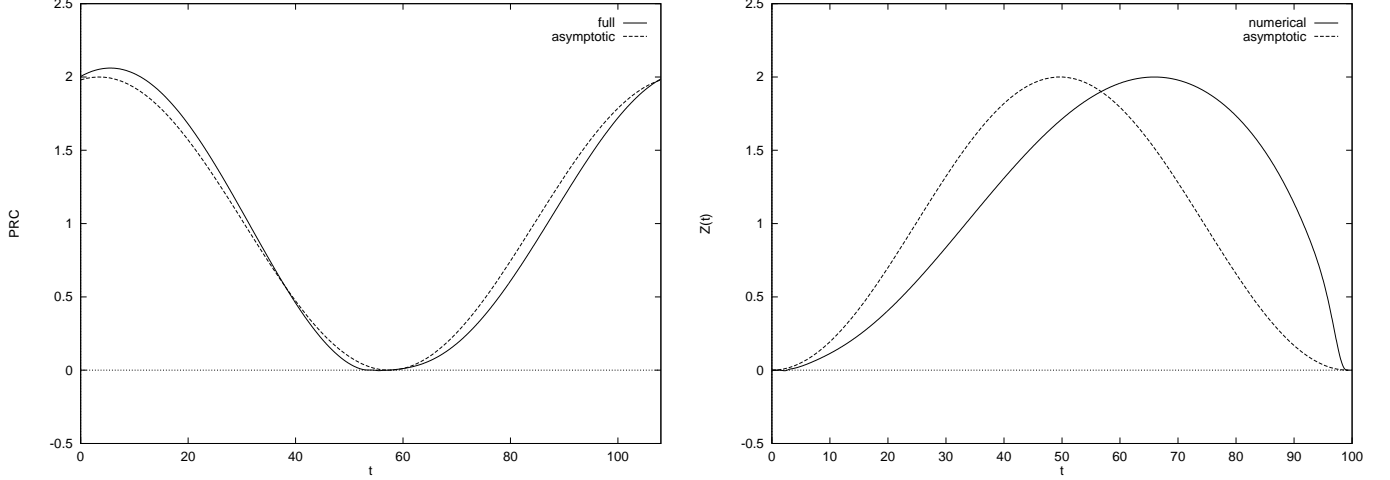


**Figure 4.** Comparison of infinitesimal response functions with the formula (2.8) for (a) Morris-Lecar model when  $I = 0.0695$  and (b) Connor model when  $I = 8.5$

together. Thus, we wish to explore the behavior of two “Type I” membrane oscillators coupled via synaptic conductances.

The synaptic current is just another current in our reduction of the full system to the phase model. Thus, the behavior of each oscillator can be expressed in terms of its “phase” (*cf* equation (2.7)) and will obey:

$$\frac{d\theta}{d\tau} = q(1 - \cos \theta) + (1 + \cos \theta) (\eta - I_{syn}(\tau)) \quad (3.1)$$

where the synaptic current is:

$$I_{syn}(\tau) = g_{syn}s(\tau)(V(\tau/\epsilon) - V_{syn}) \quad (3.2)$$

$V(t)$  is the postsynaptic potential and from (2.6) satisfies:

$$V(t) = V_0(t) + \epsilon \left( z(t) - \frac{1}{\frac{\pi}{2} - \sqrt{\eta q \epsilon t}} - \frac{1}{-\frac{\pi}{2} - \sqrt{\eta q \epsilon t}} \right) V_1. \quad (3.3)$$

where  $V_1$  is the  $V$  component of the eigenvector  $\vec{e}$ . Near criticality,  $V(t)$  spends most of its time near the rest state,  $\bar{V}$ . Therefore  $V(\tau/\epsilon) - V_{syn} \approx \bar{V} - V_{syn} \equiv -V_{eff}$  which will be positive for excitatory coupling and negative for inhibitory coupling. Thus, a pair of weakly synaptically coupled neurons

near criticality satisfies:

$$\frac{d\theta_j}{d\tau} = q_j(1 - \cos \theta_j) + (1 + \cos \theta_1) \left( \eta_j + g_{kj} s_k(\tau) V_{eff}^k \right) \quad (3.4)$$

for  $j, k = 1, 2$ . Note that this represents a new type of phase reduction model for weakly coupled nonlinear neural oscillators. The phases do not occur as differences and so the analysis is far more difficult. Furthermore, unlike phase difference models, these phase models can have equilibria corresponding to stable equilibria for the full equations (*e.g.*, by choosing  $\eta_j < 0$ ). In a sense, this is a generalization of the product coupling models proposed by Winfree (1967) and analyzed by Ermentrout and Kopell (1991) which have the form:

$$\frac{d\theta_j}{d\tau} = \omega + R(\theta_j)P(\theta_k).$$

Here  $R(\theta)$  plays the role of the response function and  $P(\theta)$  is the *pulsatile* synapse. That is, if the synapses are instantaneous functions of the presynaptic voltage (or phase) then this simple product model obtains.

All that remains is to describe the dynamics of the synaptic conductances,  $s_k(\tau)$ . There are several ways in which we can do this. If we assume that the conductances obey some type of ordinary differential equation such as (2.2) that is determined by the presynaptic potential, then we must convert these to equations that depend on the phase variables,  $\theta_j$ . An easier approach is to assume that the synaptic conductances are “alpha functions” of the form:

$$s(\tau) = \alpha^2 \tau e^{-\alpha(\tau-\tau^*)} \quad (3.5)$$

or the more general form:

$$s(\tau) = \frac{\alpha\beta}{\beta - \alpha} (e^{-\alpha(\tau-\tau^*)} - e^{-\beta(\tau-\tau^*)}). \quad (3.6)$$

Here  $\tau^*$  is the time of the presynaptic spike. Thus, we must now relate the time of a spike to the phase,  $\theta_j$ . Recall from section 2 that “firing” is equivalent to the phase variable  $\theta$  crossing  $\pi$ . Thus, an obvious strategy is to let  $\tau^*$  denote the time at which the presynaptic phase crosses  $\pi$ . However, we will generalize this to take into account certain facts about the timing of synapses. In particular, if the spike of an action potential is wide (as is the case in some relaxation-like models) then the time at which the threshold for a synaptic event is crossed and the time at which the presynaptic cell reaches its maximum can be quite different. Since the “maximum” potential

corresponds to  $\theta = \pi$  we will define  $\tau^*$  to be the time at which  $\theta = \pi - \delta$ . Here  $\delta$  is a parameter to account for the possibility that the synaptic conductance begins *before* the presynaptic voltage reaches its maximal value.

We have now reduced a pair of synaptically coupled type I membranes to a pair of phase models coupled through a synaptic conductance, (3.4). This type of coupling is difficult to analyze but has a number of modeling advantages over phase models that are derived by strict averaging. In particular, a phase difference model presumes spontaneous oscillation of all the coupled cells in absence of coupling. In (3.4) if  $\eta/q < 0$  then each uncoupled cell is incapable of spontaneously oscillating and instead has a rest state,  $\cos \theta = \frac{1+\eta/q}{1-\eta/q}$ . If coupled excitatorily and if the synapses persist for sufficiently long, the coupled system can produce rhythmic output in addition to remaining at rest. This is an example of coupling induced bistability. If both cells are started near rest, then they will return to rest. If one of them is excited past threshold, then that can cause the other cell to fire. If the synapse of cell 2 persists long enough for cell 1 to return from its refractory period (approximately the time it takes for cell 1 to go from  $\pi$  back to close to its rest state) then this will cause cell 1 to fire again and start the process over again. Figure 5 shows a picture on the  $\theta_1 - \theta_2$  torus of solutions to (3.4) in which (i) both cells are started at the same value above threshold and (ii) cell 2 starts at rest and cell 1 is above threshold. In the latter case, a spontaneous out-of-phase oscillation develops whereas in the former case, both cells return to rest.

Now suppose that both cells spontaneously oscillate so that  $\eta/q > 0$  and that both are identical. In this case, we can make a change of coordinates which reduces (3.4) to the equations:

$$\frac{d\theta_j}{d\tau} = 1 + (1 + \cos \theta_1) (gs_k(\tau)V_{eff}) \quad (3.7)$$

We can now compute a firing map function in the manner of van Vreeswijk, *et al* (1995) for this coupling. That is, we want to find periodic phase-locked solutions to (3.7). We will derive a function which indicates the possible phase-locked solutions and their stability. This is possible because the synaptic conductances are determined solely by the *times* of the spikes of the presynaptic cell and not by the value of the presynaptic phase at any other time. Let  $P$  denote the period of the phase-locked solution. Let  $\bar{s}(\tau)$  denote the synaptic time course during one cycle of the periodic solution. Suppose that cell 1 fires at  $\tau = 0$  and cell 2 fires at  $\tau = \phi P$  where  $\phi \in [0, 1)$

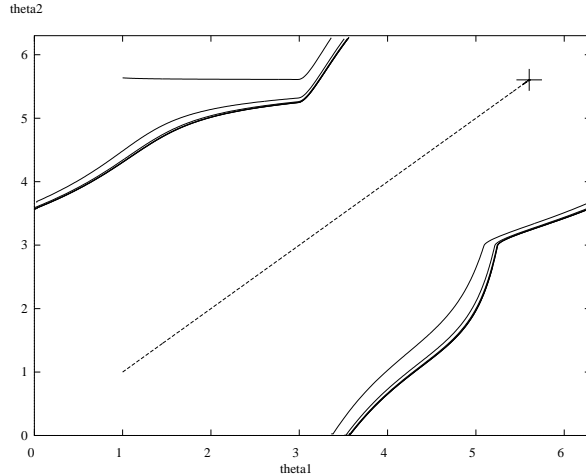


**Figure 5.** Two solutions to (3.4) showing return to rest (large cross) and spontaneous out-of-phase oscillation. Parameters are  $\eta = -0.125, q = 1, g_{jk} = 3, \delta = 0.15, \beta = 1, \alpha = 10$ .

is the relative phase. Then, cell 1 satisfies:

$$\frac{d\theta_1}{d\tau} = 1 + g\bar{s}(\tau - \phi P)(1 + \cos \theta_1)V_{eff} \quad (3.8)$$

with  $\theta_1(0) = \pi$ . Note that  $\bar{s}(\tau)$  is a known function due to the fact that once a presynaptic cell fires the time course of the synaptic response is completely determined. Call the solution to (3.8),  $\Theta(\tau; \phi)$ . Since the period is defined as the value of  $\tau$  at which  $\theta_1$  traverses  $2\pi$  we must have  $\Theta(P; \phi) = 3\pi$ . (Recall that  $\theta_1$  starts at  $\pi$ .) This gives us an equation for  $P$  as a function of  $\phi$ ,  $P = Q(\phi)$ . A similar argument used for cell 2 shows that its period must satisfy  $P = Q(-\phi)$ . Since the periods for a phase-locked solution must be the same, we must have  $G(\phi) \equiv Q(\phi) - Q(-\phi) = 0$  which determines the possible phase-locked solutions. Two immediate solutions to  $G(\phi) = 0$  are  $\phi = 0$ , synchrony, and  $\phi = 1/2$  which is the antiphase solution. A necessary and sufficient condition for stability of a phase-locked solution,  $\bar{\phi}$  is that  $Q'(\bar{\phi}) > 0$  and equivalently since  $G$  is twice the odd part of  $Q$  that  $G'(\bar{\phi}) > 0$ . To see this, suppose that cell 2 fires a bit later than  $\bar{\phi}$ . Then the period of the first cell must lengthen in to allow the second cell to catch up. That is,  $Q'(\bar{\phi}) > 0$ . For the integrate and fire model analyzed by van Vreeswijk, *et al* the function  $Q(\phi)$  can be explicitly determined. For the present model, we must resort to numerical solutions.

Figure 6 shows the firing map  $G(\phi)$  for  $g = V_{eff} = 1, \delta = 0, \alpha = \beta = a$  as a function of  $a$  the rate of the synapse. It appears that no matter what the rate of the synapse, the synchronous solution is unstable and the anti-phase oscillation is stable. The opposite occurs for inhibition ( $V_{eff} < 0$ ). Hansel, *et al* (1995) as well as van Vreeswijk, *et al* (1995) found that for sufficiently fast excitation, synchrony became stable. We can obtain a similar result in this model if we take into account the finite width of the action potential and thus set  $\delta$  to some small positive value. Figure 7 shows the firing map for both excitatory and inhibitory coupling as a function of the synaptic rate. Consider excitatory coupling. As the synaptic rate increases, the synchronous state stabilizes and there is bistability between the synchronous and the anti-phase solution. For very fast synapses, the anti-phase solution becomes unstable and synchrony is the only stable state. A similar scenario occurs with inhibitory coupling however in this case fast synaptic interactions result in the stability of the anti-phase state. One should not place too much emphasis on the details of the bifurcation structure as this is quite dependent on the choice of the synaptic gating function  $s(t)$ . Thus, the picture for inhibitory coupling in figure 7 is the same as that in van Vreeswijk, *et al* but for excitatory coupling our diagram is different. For the excitatory integrate and fire model analyzed by van Vreeswijk, *et al* and for the weakly excitatory coupled Connor model considered by Hansel, *et al* (1995) the transition from stable anti-phase to stable synchrony occurs via an intermediate regime where neither is stable. Instead there is a stable nonzero phase-lag between the the oscillators.

### 3.1 Some comments on averaging.

The averaging method can be applied to a pair of oscillators as long as the coupling is very weak compared to the period of the oscillation. Since the oscillators we are describing here have very long periods, the coupling must be *extremely* weak in order to rigorously apply averaging. Nevertheless, we can get some useful insights into the the global picture for type I membranes by looking at the averaged equations. Let  $g$  be small in (3.4) and let  $Z(\theta) = (1 + \cos \theta)$  denote the response function to lowest order. Then one can average the phase equations and we obtain the following equation for the phases,  $\theta_j$

$$\frac{d\theta_1}{d\tau} = 1 + gH(\theta_2 - \theta_1) \quad (3.9)$$



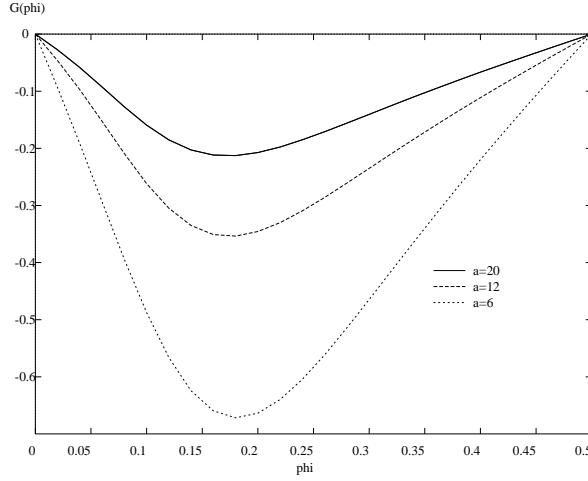


**Figure 6.** The firing map  $G(\phi)$  for excitatory coupling,  $g = V_{eff} = 1$ ,  $\delta = 0$ ,  $\alpha = \beta = a$  for various values of  $a$  the rate of the synapse. Only the out-of-phase solution is stable.

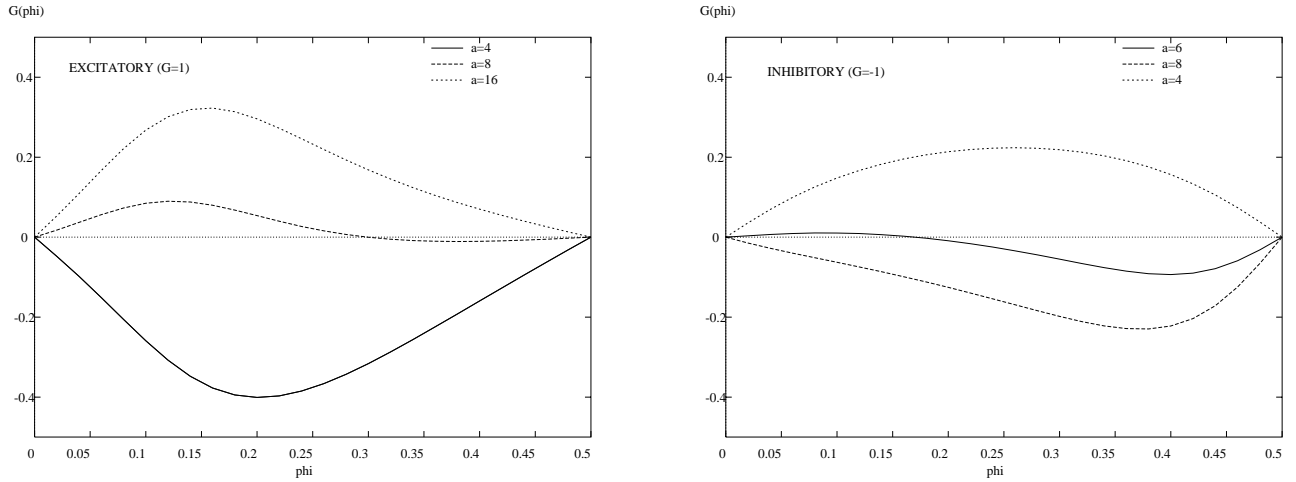


**Figure 7.** The firing map for excitatory and inhibitory coupling when the synapse starts slightly before the peak of the spike ( $\delta = 0.05$ ). Left-hand panel is excitatory coupling ( $V_{eff} = 1$ ) and right panel is inhibitory ( $V_{eff} = -1$ .) All other parameters as in Figure 6.

$$\frac{d\theta_2}{d\tau} = 1 + gH(\theta_1 - \theta_2) \quad (3.10)$$

where

$$H(\theta) = V_{eff} \frac{1}{2\pi} \int_0^{2\pi} Z(t)s(t + \theta)dt. \quad (3.11)$$

Letting  $\phi = \theta_2 - \theta_1$ , we can subtract (3.9) from (3.10) and obtain:

$$\frac{d\phi}{d\tau} = g(H(-\phi) - H(\phi)) = g\Gamma(\phi).$$

The zeros of  $\Gamma(\phi)$  are the phase-locked solutions and they are stable as long as  $\Gamma'(\phi) < 0$  or equivalently,  $H'(\phi) > 0$ . Note that  $\Gamma$  is proportional to the odd part of the function  $H$ . Now, for our lowest order model,  $Z(t) = 1 + \cos t$  so that  $H$  must be of the form  $H(\theta) = a_0 + a_1 \cos \theta + b_1 \sin \theta$  and thus  $\Gamma(\phi) = -2b_1 \sin \phi$ . The first thing to note is that there are only two possible phase-shifts (zeros of  $\Gamma$ ) and they are  $\phi = 0$  and  $\phi = \pi$ . Thus, no matter what  $s(t)$  is, the solutions to the averaged equations have no other possible phase-lags. The reason that Hansel, and others have found these intermediate phase-lags in their averaged equations is that the response function  $Z(\theta)$  has higher Fourier components. Indeed, our response function,  $1 + \cos \theta$  is only the lowest order term in asymptotic expansion; higher order terms will generally contain modes such as  $\cos 2\theta$ . The coefficients of these higher order determine the nature of the transition from synchrony to anti-phase as the synaptic rate varies. A detailed analysis of this transition is given in van Vreeswijk, *et al* (1995).

## 4 Discussion and Conclusions

The calculations in the previous section suggest the general picture for a pair of weakly coupled type I membrane oscillators as a function of the persistence of excitatory synapses and inhibitory synapses. For slow enough synapses and excitatory interactions, the synchronous solution is unstable and the anti-phase solution is stable. Under some circumstances, as the synapses speed up, the synchronous solution stabilizes and the anti-phase solution loses stability. The reverse is true for inhibitory interactions. The mechanism for change of stability (if it occurs) depends on higher order details of the model.

We have shown that neural oscillators that arise from Type I excitability, (that is via a saddle-node bifurcation on a circle rather than via a Hopf bifurcation) have type I or non-negative phase resetting curves. Thus, we have

connected the local oscillator mechanisms to the behavior of such oscillators when connected to others.

A natural question is whether oscillations that arise through Hopf bifurcations have type II phase-resetting properties, that is, is the phase resetting curve positive for some phases and negative for others (*cf* Figure 3b,c). For a supercritical Hopf bifurcation (that is, a stable *small amplitude* oscillation emanating from a fixed point) this question is easy to answer. Near the bifurcation point, the oscillation is sinusoidal and the adjoint is easily computed (see Ermentrout and Kopell, 1984) to be of the form:

$$Z(t) = Z_x \cos \omega t + Z_y \sin \omega t$$

where  $Z_x, Z_y$  are constant vectors that depend on the properties of the membrane and  $\omega$  is the natural frequency. Thus, we can say that for membranes that undergo a supercritical Hopf bifurcation, the phase response function is sinusoidal and is therefore a type II phase resetting curve. (Many membranes can be put into this regime at high enough temperatures, but it is normally unusual.)

## References

- [1] J. A. Connor, D. Walter, and R. McKown, 1977, Neural repetitive firing: modification of the Hodgkin-Huxley axon suggested by experimental results from crustacean axons, *Biophysical J.*, **18**, 81-102.
- [2] A. Destexhe, Z. Mainen, T. Sejnowski, 1994, Synthesis of models for excitable membranes, synaptic transmission and neuromodulation using a common kinetic formulation, *J. Comput. Neurosci.* 1:195-230.
- [3] G.B. Ermentrout and N. Kopell, 1984, Frequency plateaus in a chain of weakly coupled oscillators I., *SIAM J. Math. Anal.* 15:215-237
- [4] G.B. Ermentrout and N. Kopell, 1986, Parabolic bursting in an excitable system coupled with a slow oscillation, *SIAM J. Appl. Math.*, **46** 233-253.
- [5] G.B. Ermentrout and N. Kopell, 1991, Multiple pulse interactions and averaging in systems of coupled neural oscillators, *J. Math. Bio.* **29**,195-217.

- [6] D. Hansel, G. Mato, and C. Meunier, 1993, Phase reduction in neural modeling, in *Functional Analysis of the Brain based on Multiple-Site Recordings, October 1992, Concepts in Neuroscience* **4**, 192-210.
- [7] D. Hansel, G. Mato, and C. Meunier, 1995, Synchrony in excitatory neural networks, *Neural Computation*, **7**,307-335.
- [8] A.L. Hodgkin, 1948, The local electric changes associated with repetitive action in a non-medulated axon, *J. Physiol. (London)*, **117**, 500-544.
- [9] Y. Kuramoto, 1984, *Chemical Oscillations, Waves, and Turbulence*, Springer-Verlag, New York.
- [10] J.R. Rinzel and G.B.Ermentrout, 1989, Analysis of neural excitability and oscillations, in *Methods in Neuronal Modeling*, C. Koch and I. Segev, eds, MIT Press, Cambridge, 135-169.
- [11] C. Morris and H. Lecar, 1981, Voltage oscillations in the barnacle giant muscle fiber, *Biophys. J.*, **35**, 193-213.
- [12] A. Nayfeh, 1973, *Perturbation Methods*, Wiley, New York.
- [13] C. van Vreeswijk, L.F. Abbott, and G. B. Ermentrout, 1995, When inhibition, not excitation synchronizes neural firing, *J. Comput. Neurosci.*, **1**, 313-322.
- [14] X.J. Wang, D. Golomb, and J. Rinzel, 1995, Emergent spindle oscillations and intermittent burst firin in a thalamic model: Specific neuronal mechanisms, *Proc. Natl. Acad. Sci, USA* **92** 5577-5581.
- [15] A.T. Winfree, 1967, Biological rhythms and the behavior of populations of coupled oscillators, *J. Theoretical Biology* **16**, 15-42.

### **Appendix A: Numerical simulation parameters**

The models used in this paper are the Hodgkin-Huxley model, the Connor model, and the dimensionless Morris-Lecar equations. All equations were integrated using a 4th order Runge-Kutta method on the software XPP. Frequency plots were computed using a modified version of AUTO incorporated into XPP. The response functions and phase interaction functions were also computed using XPP. All simulation code is available from the author at `bard@poincare.math.pitt.edu`.

The Hodgkin-Huxley equations used here are:

$$\begin{aligned}
C \frac{dV}{dt} &= I - 120mh^3(V - 50) - 36n^4(V + 77) - 0.3(V + 54.4) \\
\frac{dm}{dt} &= \alpha_m(V)(1 - m) - \beta_m(V)m \\
\frac{dh}{dt} &= \alpha_h(V)(1 - h) - \beta_h(V)h \\
\frac{dn}{dt} &= \alpha_n(V)(1 - n) - \beta_n(V)n
\end{aligned}$$

where

$$\begin{aligned}
\alpha_m(V) &= .1 * (V + 40)/(1 - \exp(-(V + 40)/10)) \\
\beta_m(V) &= 4 * \exp(-(V + 65)/18) \\
\alpha_h(V) &= .07 * \exp(-(V + 65)/20) \\
\beta_h(V) &= 1/(1 + \exp(-(V + 35)/10)) \\
\alpha_n(V) &= .01 * (V + 55)/(1 - \exp(-(V + 55)/10)) \\
\beta_n(V) &= .125 * \exp(-(V + 65)/80).
\end{aligned}$$

For the simulations in this paper,  $I = 12$ .

The version of the Connor model we use here is the same as that used by Hansel, et.al. (except for  $a_\infty(V)$  which is incorrectly defined in their paper.)

$$\begin{aligned}
C \frac{dV}{dt} &= I - 120mh^3(V - 55) - 20n^4(V + 72) - 0.3(V + 17) + 47.7a^3b(V + 75) \\
\frac{dm}{dt} &= \alpha_m(V)(1 - m) - \beta_m(V)m \\
\frac{dh}{dt} &= \alpha_h(V)(1 - h) - \beta_h(V)h \\
\frac{dn}{dt} &= \alpha_n(V)(1 - n) - \beta_n(V)n \\
\frac{da}{dt} &= \frac{a_\infty(V) - a}{\tau_a(V)} \\
\frac{db}{dt} &= \frac{b_\infty(V) - b}{\tau_b(V)}
\end{aligned}$$

where

$$\alpha_m(V) = .1 * (V + 29.7)/(1 - \exp(-(V + 29.7)/10))$$

$$\begin{aligned}
\beta_m(V) &= 4 * \exp(-(V + 54.7)/18) \\
\alpha_h(V) &= .07 * \exp(-(V + 48)/20) \\
\beta_h(V) &= 1/(1 + \exp(-(V + 18)/10)) \\
\alpha_n(V) &= .01 * (V + 46.7)/(1 - \exp(-(V + 46.7)/10)) \\
\beta_n(V) &= .125 * \exp(-(V + 56.7)/80) \\
a_\infty(V) &= (.0761 * \exp((V + 94.22)/31.84)/(1 + \exp((V + 1.17)/28.93)))^{.3333} \\
\tau_a(V) &= .3632 + 1.158/(1 + \exp((V + 55.96)/20.12)) \\
b_\infty(V) &= 1/(1 + \exp((V + 53.3)/14.54))^4 \\
\tau_b(V) &= 1.24 + 2.678/(1 + \exp((V + 50)/16.027)).
\end{aligned}$$

For the simulations in this paper,  $I = 8.5$ .

The dimensionless Morris-Lecar equations are given in section 1. The parameters used for “Type I” excitability dynamics are:  $g_I = .5, g_K = 2, g_{Ca} = 1.33, V_1 = -.01, V_2 = 0.15, V_3 = 0.1, V_4 = 0.145, V_{Ca} = 1, V_K = -.7, V_L = -.5$  with  $I = 0.0695$ . The parameters for “Type II” dynamics are as above with the exception of  $g_{Ca} = 1.1, V_3 = 0.0, V_4 = 0, 3, \phi = 0.2$  and  $I = 0.25$ .

## Appendix B: Computation of the response function

**Scalar phase model.** We compute the response function for a scalar phase model of the form:

$$\frac{d\theta}{dt} = f(\theta) + g(\theta) \cdot S(t)$$

where  $S(t)$  is the stimulus inducing the phase-shift. Let  $\theta_0(t)$  satisfy

$$\frac{d\theta_0}{dt} = f(\theta_0(t)).$$

Since this models a phase oscillator,  $\theta_0$  monotonically increases (or decreases) in time since  $f$  is strictly positive (negative). Thus, we can introduce a new phase-variable,  $\psi$  defined by,  $\theta(t) = \theta_0(\psi)$ .  $\psi$  satisfies:

$$\frac{d\psi}{dt} = 1 + \frac{g(\theta_0(\psi))}{\theta_0'(\psi)} S(t) \equiv Z(\psi) S(t).$$

The expression multiplying  $S(t)$  is the response function. For our dynamics,  $f(\theta) = q(1 - \cos \theta) + ci(1 + \cos \theta)$  and  $g(\theta) = (1 + \cos \theta)$  where  $ci > 0$ .

It is then an elementary application of trigonometric identities to see that  $Z(\theta) = K(1 + \cos \theta)$  as required.

**Numerical computation of the response function.** It can be shown (Ermentrout and Kopell, 1991) that the response function,  $Z(t)$  is the adjoint eigenfunction for the linearization of the differential equations about the stable limit cycle. That is, let  $X(t)$  satisfy:

$$\frac{dX}{dt} = F(X)$$

and suppose that  $X(t)$  is orbitally stable. The adjoint to the linearization satisfies:

$$\frac{dZ(t)}{dt} = -DF(X(t))^T Z(t) \tag{4.1}$$

where  $DF(X(t))$  is the Jacobi matrix of  $F$  evaluated at  $X(t)$  and  $A^T$  denotes the transpose of  $A$ . Since  $X(t)$  is orbitally stable, then integration in *forward* time of the linearized equations will always relax to a periodic orbit. Thus, to find the periodic solution to (4.1), we start with random initial conditions and integrate *backward* in time over several periods. This will relax to the adjoint,  $Z(t)$  which is then normalized so that

$$\frac{1}{T} \int_0^T Z(t) \cdot X'(t) dt = 1.$$

This method of computing the adjoint was suggested to the author by Graham Bowtell. The author's software package includes this algorithm so that all these calculations are readily automated. Error is introduced in the numerical calculations in two ways. The computation of the Jacobi matrix is done numerically so for sharp spikes error can be introduced. Integration of the linear equations also produces the usual numerical errors.